Available online at www.sciencedirect.com
ScienceDirect
Applied Radiation and Isotopes 65 (2007) 401–406
Applied Radiation and Isotopes
www.elsevier.com/locate/apradiso

Calibration of a ^{137}Cs γ-ray beam irradiator using large size chambers

R. Minniti*, S.M. Seltzer

National Institute of Standards and Technology, Ionizing Radiation Division, 100 Bureau Drive Building 245, Gaithersburg, MD 20899-8460, USA

Received 21 July 2006; received in revised form 13 October 2006; accepted 16 October 2006

Abstract

A ^{137}Cs γ-ray beam irradiator has been calibrated in terms of air kerma using large size chambers. The available air-kerma rates range between 1.8 μGy/h (0.2 mR/h) and 5.3 mGy/h (0.6 R/h). Large-volume chambers were used to characterize the source in terms of the radiation quantity air kerma (and exposure). Two types of chambers with significantly different characteristics and energy responses were used. This work shows that very good agreement can be obtained between the measurements performed with such different types of chambers. An agreement of 0.3% is observed between chambers even for the lowest air-kerma rates measured.
Published by Elsevier Ltd.

Keywords: Ionization chamber; Cs-137; γ-ray; Scattered radiation; Secondary standard; Calibration coefficient; Air kerma

1. Introduction

A total of seven ^{137}Cs and ^{60}Co γ-ray irradiators are routinely used by the Radiation Interactions and Dosimetry Group at the National Institute of Standards and Technology (NIST) in support of the calibration program for disseminating the primary standards for air kerma (Minniti et al., 2006; Lamperti and O'Brien, 2001; Pibida et al., 2005). These facilities provide reference radiation γ-ray beams that have been characterized in terms of the radiation quantities air kerma and exposure using a suite of six graphite cavity air ionization chambers (Loftus and Weaver, 1974; Seltzer and Bergstrom, 2003). These chambers constitute the NIST *primary standard* instruments for the measurement of air kerma from γ-ray beams. These existing *primary standard calibration facilities* provide a broad range of air-kerma rates. Currently, the lowest air-kerma rate available for the ^{137}Cs γ-ray beams is approximately 4.4 mGy/h (0.5 R/h). Here, we report the development of a new calibration range that allows extending the air-kerma rate values down to approximately 1.8 μGy/h (0.2 mR/h).

The reference radiation γ-ray beams in the new facility were characterized using *secondary standard* ionization chambers of large volumes. The calibration range allows to position radiation detector equipment between 1 and 4 m from the source accurately. The source output was measured with four large-volume chambers that had been calibrated against the primary standard in the existing NIST primary standard calibration facilities. Large-volume chambers allow the measurement of low air-kerma rates. Chambers of two types with significantly different characteristics were used. The chambers of the first type are pressurized and sealed to the atmosphere. Their walls are made of stainless steel in order to contain the pressurized gas. The chambers of the second type are open to the atmosphere and have air-equivalent plastic walls. As a result of these different characteristics, the energy response of these chambers is very different over a photon energy range between 30 and 662 keV. The response of the air-equivalent plastic-wall chambers is constant within 5% over the entire energy range. The response of the pressurized chambers is relatively constant between 300 and 662 keV, too; however, it drops drastically below 300 keV (the difference between the responses at 300 and 100 keV is approximately 30%).

In this work, we used these two types of chambers to characterize the output of the source down to air-kerma rates as low as 1.8 μGy/h (0.2 mR/h). It was found that,

*Corresponding author. Tel.: +1 301 975 5586; fax: +1 301 869 7682.
E-mail addresses: rminniti@nist.gov, ronaldo.minniti@nist.gov (R. Minniti).

0969-8043/$ - see front matter Published by Elsevier Ltd.
doi:10.1016/j.apradiso.2006.10.008

despite the significantly different properties of the chambers, the lower air-kerma rates measured with them agree within 0.3%. For air-kerma rates above 8.78 μGy/h (1 mR/h), the differences become smaller.

There are many *secondary standard calibration facilities* throughout the world that are similar to the newly developed calibration facility described in this report. They provide air-kerma measurements traceable to primary standard calibration facilities (IAEA, 2005). In this paper, we report differences that can be expected in the measurements of air kerma with large volume chambers. Secondary standard facilities elsewhere may benefit from the data reported here.

A brief section on the calibration of secondary standard large-volume chambers is included in addition to a description of the calibration range and the measurement methods used. This is followed by a discussion of the results and conclusions.

2. Calibration of secondary standard large-volume chambers

Four large-volume chambers were calibrated against the primary standard in one of the existing NIST ^{137}Cs γ-ray primary standard calibration facilities. For each chamber, we determined an air-kerma calibration coefficient

$$N_\mathrm{K} = \frac{\dot{K}_\mathrm{p}}{I_\mathrm{p}}, \tag{1}$$

where $\dot{K}_\mathrm{p}$ is the air-kerma rate of the NIST reference radiation beam in the primary standard calibration facility (determined by applying a decay correction to the original air-kerma rate value) and I_p is the ionization current measured with one of the large-volume chambers in the primary standard calibration facility. The value of the ionization current I_p includes corrections to account for ion-recombination effects (Boag, 1987; Boutillon, 1998; Zankowski and Podgorsak, 1998) and for deviations of the ambient temperature and pressure from the NIST reference conditions of 22 °C and 101.325 kPa (1 atm), respectively (Lamperti and O'Brien, 2001).

Once all four secondary standard large-volume chambers were calibrated in the NIST primary standards calibration facility, they were used to determine the air-kerma rates at various distances from the ^{137}Cs source in the new secondary standard calibration facility. The air-kerma rates $\dot{K}$ measured with each chamber were determined using the expression

$$\dot{K} = N_\mathrm{K} \cdot I, \tag{2}$$

where N_K is the calibration coefficient for a given chamber and I is the measured ionization current in the secondary standard calibration facility. The value of the ionization current included a correction for recombination loss. In the case of chambers open to atmosphere, an additional correction was included to account for deviations of the ambient temperature and pressure from the NIST reference conditions.

3. Materials and methods

The new secondary standard calibration facility utilizes a ^{137}Cs irradiator made by Shepherd and Associates.[1] The irradiator is essentially a cylindrically shaped tower that has five ^{137}Cs sources mounted on a rod. The rod can slide vertically to position a single source, at a given time, in front of a collimator opening located approximately in the center of the tower. In the closed position, the sources are stored in the heavily shielded bottom part of the tower. Three of these sources were used in this work. For identification purposes only, each of these three sources will be referred to throughout the text of this manuscript using the manufacturer's nomenclature, i.e., by their nominal activities of 15 mCi, 300 mCi and 6 Ci (on October 15, 1994). The beam axis is located at a height of 1.4 m from the floor. The collimator opening provides a square radiation field of approximately 28 cm × 28 cm (defined by the 95% iso-intensity contour) at a distance of 1 m from the source.

A track system, designed and built at NIST, lies along the floor parallel to the beam center axis and allows for accurate positioning of radiation instruments at the distances between 60 and 430 cm from the source. Two lasers are used to align the instruments at the desired source-to-detector distance and beam axis height. A mounting stand, built of bakelite to minimize scattered radiation, is used for mounting the ionization chambers.

The data acquisition system is composed of an electrometer and a temperature and pressure transducers. A computer program, developed in Visual Basic, is used to acquire and simultaneously analyze the charge integrated over a given period of time and the temperature and pressure in the vicinity of the chamber.

Four large-volume spherical ionization chambers were used. The chamber specifications are summarized in Table 1. Two of the chambers were pressurized ionization chambers (PICs) and will be referred to throughout the text as PIC1 and PIC2. Both chambers are of the same type. The other two chambers are non-pressurized and are open to the atmosphere. These chambers will be referred to throughout the text by the manufacturer's models identification, i.e. A6 and A7. A bias of 1000 V was applied to the chambers A6 and A7, while 700 V was applied to the chambers PIC1 and PIC2. In all cases, only negative charge was collected.

All four chambers were calibrated in terms of air kerma (and exposure) at a higher air-kerma rate of approximately 4.4 mGy/h (0.5 R/h) in one of the existing NIST ^{137}Cs reference beams. An air-kerma calibration coefficient, N_K, was obtained for each secondary standard chamber. Each

[1]Certain commercial equipment, instruments, and materials are identified in this work in order to specify adequately the experimental procedure. Such identification does not imply recommendation or endorsement by NIST, nor does it imply that the material or equipment identified is the best available for the purposes described in this work.

Table 1
Chamber specifications[a]

Name	A6	A7	PIC1 and PIC2
Make	Exradin	Exradin	LND
Volume (L)	0.8	3.3	8
Outer diameter (cm)	11.4	19.6	25.4
Wall material	C552 Plastic	C552 Plastic	Stainless Steel
Wall thickness (mm)	3	6	3
Gas	Air	Air	Argon
Gas pressure	Atmospheric	Atmospheric	26.9 atm

[a]Certain commercial equipment, instruments, and materials are identified in this work in order to specify adequately the experimental procedure. Such identification does not imply recommendation or endorsement by NIST, nor does it imply that the material or equipment identified is the best available for the purposes described in this work.

chamber was then used to determine the air-kerma rates in the new calibration range by evaluating Eq. (2). The air-kerma rate values were determined for a total of seven source-detector distances for each of the three ^{137}Cs sources.

The air-kerma rate obtained with a given chamber at a single measurement point, i.e. at a given source-to-detector distance, was determined from the average of multiple measurements. Typical integration times for a single measurement varied between 60 and 300 s. The values of the internal capacitors of the electrometer were between 20 nC and 2 μC for the lowest and highest current, respectively. A group of multiple measurements with the same setup was repeated within a given day and also over different days over a period of six months to assess the reproducibility of different measurement setups with a given chamber. The measured values reproduced quite well with all of the chambers, within 0.2%.

4. Results and discussion

Fig. 1 shows a comparison of the values of the air-kerma rates obtained with each one of the four chambers relative to the average value. The average air-kerma rate was computed using the values from a subset of all four chambers. For example, the average air-kerma rate at a distance of 2.6 m was obtained from the air-kerma rate values measured using the chambers A7, PIC1 and PIC2. Note that the air-kerma rate values shown in the figure were obtained using the 15 and 300 mCi sources (for clarity, the air-kerma rate values obtained using the 6 Ci source are not shown in the figure). The data points corresponding to the air-kerma rates measured with the 15 mCi source are represented by the open symbols, and the data points corresponding to the air-kerma rates measured with the 300 mCi source are represented by the solid symbols. For a given source, the figure shows the air-kerma rates measured at a total of five source-detector distances with several of the chambers. One can see that the

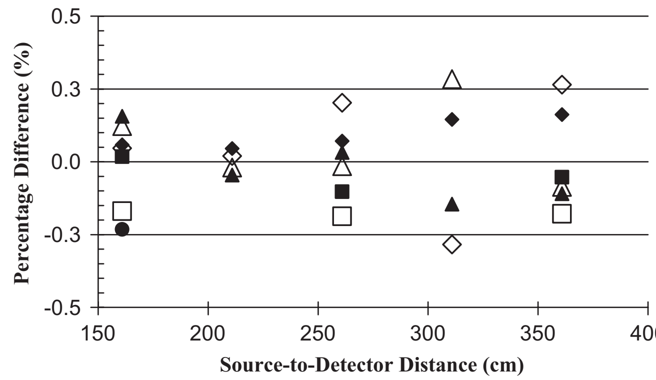

Fig. 1. Percentage difference between the air-kerma values obtained for each chamber and the average air-kerma value resulting from the chamber measurements (see text). The open symbols represent the data obtained from the 15 mCi source, and the solid symbols represent the data obtained from the 300 mCi source. Each data point represents measurements made with the following chambers: PIC1 (squares), PIC2 (diamonds), A7 (triangles), and A6 (circles).

spread in the air-kerma rate values relative to the average value measured with the 300 mCi source (solid symbols) is smaller than that obtained with the 15 mCi source (open symbols). In all cases, i.e. for all three sources used in this work (with nominal activities of 15 mCi, 300 mCi and 6 Ci), the differences between the value of the air-kerma rate obtained with each chamber and the average value did not exceed 0.30%. This result is interesting because pressurized chambers are better suited for the measurements of lower air-kerma rates from ^{137}Cs beams. In principle, the drastically different energy response of these chambers relative to the non-pressurized chambers could lead one to believe that the differences expected in the air-kerma rate measurements between chambers must be larger. The results show that, despite the significantly different energy response for the different types of chambers, a very good agreement at the 0.3% level can be expected between chambers.

The measured average air-kerma rate values, $\bar{\dot{K}}$, as a function of source-to-detector distance, x, were fit for each of the three sources using the following expression:

$$\bar{\dot{K}} = \frac{A}{(x+E)^2} + \frac{B}{(x+E)} + C + D(x+E), \quad (3)$$

where A, B, C, D, and E are fitting parameters.

Eq. (3) was derived by considering the inverse square law for the air-kerma rate from a point source modified to include attenuation and buildup in air (Attix, 1986). Although Eq. (3) is based on a crude mathematical model of the radiation physics involved, it cannot be considered accurate from a physical point of view because other processes are being ignored. Therefore, no physical interpretation should be given to the fitting parameters obtained. The equation and its fitting parameters should only be used to predict the values of air-kerma rates for the range of source-to-detector distances for which measurements have been made, i.e., between 1 and 4 m.

Table 2
Fitting parameters for all three sources (the reference date for the fitting parameters is April 1, 2006)

Source ID	A (Gy h^{-1} cm^2)	B (Gy h^{-1} cm)	C (Gy h^{-1})	D (Gy h^{-1} cm^{-1})	E (cm)
15 mCi	2.7623×10^{-1}	8.7002×10^{-6}	-1.2817×10^{-7}	2.6735×10^{-10}	0.55
300 mCi	6.9459	-3.8030×10^{-5}	-2.5351×10^{-6}	5.9597×10^{-9}	0.79
6 Ci	$1.2645\times10^{+2}$	-7.6981×10^{-3}	-5.4048×10^{-5}	1.4535×10^{-7}	1.77

Five significant digits are shown for each parameter to prevent rounding errors when the parameters are used in calculations; they do not represent, however, the level of accuracy of the predicted air-kerma values.

Table 3
Average air-kerma rate values for several source-to-detector distances and for all three sources with initial activities of 15 mCi, 300 mCi and 6 Ci

Source ID	15 mCi		300 mCi		6 Ci	
Distance (cm)	Measured rate (Gy/h)	Percentage difference (%)	Measured rate (Gy/h)	Percentage difference (%)	Measured rate (Gy/h)	Percentage difference (%)
100	2.731×10^{-5}	0.00	6.815×10^{-4}	0.00	1.209×10^{-2}	0.00
161	1.057×10^{-5}	0.00	2.638×10^{-4}	0.05	4.701×10^{-3}	0.00
211	6.151×10^{-6}	−0.05	1.537×10^{-4}	−0.11	2.737×10^{-3}	−0.01
261	4.012×10^{-6}	0.11	1.002×10^{-4}	0.14	1.787×10^{-3}	0.00
311	2.839×10^{-6}	−0.30	7.072×10^{-5}	−0.02	1.261×10^{-3}	−0.06
361	2.104×10^{-6}	0.16	5.260×10^{-5}	0.02	9.382×10^{-4}	0.06
400	1.724×10^{-6}	−0.07	4.305×10^{-5}	−0.11	7.685×10^{-4}	0.00

Also shown are the percentage differences between the measured and fitted air-kerma values (the reference date for the air-kerma rate values is April 1, 2006).

Table 2 shows the values of the fitting parameters from Eq. (3) obtained for each of the three sources. The reference date for the shown parameters is April 1, 2006, and air-kerma rates predicted for subsequent dates may be obtained by applying the corresponding decay correction. The value of the half-life for ^{137}Cs used here is 30.07 years (standard uncertainty of 0.03 years) (Kafala et al., 1994; Sonzogni, 2006). Table 3 shows the measured average air-kerma rates at several source-to-detector distances for each of the three sources. Table 3 also shows the differences obtained between the air-kerma rate values predicted using Eq. (3) and the measured air-kerma rates. As shown in the table, the differences are very small and, in most of the cases, do not exceed 0.1%.

The value of the relative expanded uncertainty for the highest measured air-kerma rate is estimated to be 1% for both types of chambers, i.e., for the non-pressurized chamber and the pressurized chambers. A typical uncertainty analysis is shown in Table 4 for one of the chambers at a measured air-kerma rate of 5.3 mGy/h (0.6 R/h). The uncertainty components listed in Table 4 are grouped, for a given chamber, in two columns: Type A and Type B. Type A evaluations result from a statistical analysis, while Type B evaluations are based on scientific judgment (Taylor and Kuyatt, 1994; ANSI/NCSL, 1997). The relative expanded uncertainty was calculated as two times the square root of the sum of squares of the experimentally measured relative standard deviations for the Type A components, and of the estimated relative standard deviations for all other (Type B evaluated) uncertainty components. This value is considered to have approximately the significance of a 95% confidence interval (Taylor and Kuyatt, 1994; ANSI/NCSL, 1997).

Table 4
Uncertainty analysis for an air-kerma rate of 5.3 mGy/h (0.6 R/h) measured with the A7 chamber

Relative standard uncertainty components, u_j	Type A evaluation	Type B evaluation
Calibration coefficient, N_K	0.1	0.4
Net ionization current, I (rate dependent)	0.1	
Reproducibility		0.20
Distance		0.05
Chamber rotational dependence		0.02
Air density correction		0.06
Quadratic sum, $\sqrt{\sum_j u_j}$	0.14	0.45
Relative combined uncertainty of the air-kerma rate	0.48	
Relative expanded uncertainty of the air-kerma rate ($k=2$)	0.95	

The relative uncertainties are expressed in %.

The value of the measurement uncertainties for the lower measured air-kerma rates is significantly different for the two types of chamber used. For example, for a measured air-kerma rate of 1.8 μGy/h (0.2 mR/h) the relative expanded uncertainty of the air-kerma rate is 1.1% and 2.6% for the PIC and A7 chambers respectively. This difference is mainly driven by the value of the relative standard uncertainty of the net ionization current, u_I/I, listed in Table 4. The net ionization current, I, is determined as

$$I = I_S - I_B, \tag{4a}$$

where I_S is the value of the ionization current measured in the presence of radiation (source exposed) and I_B is the value of the background current, i.e. the value of the chamber current in the absence of radiation (source shielded). Therefore, the relative standard uncertainty of the net ionization current can be expressed as

$$\frac{u_I}{I} = \frac{\sqrt{u_S^2 + u_B^2}}{I}, \tag{4b}$$

where u_S is the standard uncertainty of the ionization current I_S and u_B is the standard uncertainty of the background current I_B. For low air-kerma rates of the order of 1.8 μGy/h (0.2 mR/h), a typical value of the net ionization current I obtained with the A7 chamber is 6.0×10^{-14} C/s, with a standard uncertainty of $u_I = 0.7 \times 10^{-15}$ C/s. This results in a relative standard uncertainty for the ionization current of 1.2%. The corresponding values obtained with the pressurized ion chambers are $I = 6.0 \times 10^{-12}$ C/s and $u_I = 16 \times 10^{-15}$ C/s, resulting in a relative standard uncertainty for the net ionization current of 0.3%.

An estimate of the effect of the radiation field non-uniformity within the chamber volume was made using the theory developed by Kondo and Randolf (1960). This effect can be quite large, reaching a few percent for large-volume chambers located very near the source. However, the measurements with the A7 chamber reported here were performed at distances between 1.0 and 4 m. The magnitude of the Kondo-Randolf correction determined at the closest distance with the A7 chamber is 0.3%; it is smaller for greater distances. The measurements with the pressurized ion chambers were made at distances larger than 1.6 m. The value of the Kondo–Randolf correction at the closest distance of 1.6 m is 0.2%; for longer distances, these corrections become even smaller.

Radiation scattered into the chambers from the room walls and source collimation was assessed using the shadow-shield technique (Verhaegen et al., 1992). A shield made of lead with a cross sectional dimension of 20 cm × 10 cm and thickness of 10 cm was positioned between the source and the chamber to block the primary beam. In this way, only scattered radiation is detected by the chamber. The fraction of the scattered beam to the total was measured at several distances from the source for all three sources, and the results are shown in Fig. 2. As shown in the figure the scattered radiation increases with distance from 1.5% for the shortest distance up to 3.0% at the longest distance. The measurements were made with the A7 chamber and one of the pressurized chambers. The results obtained with the two different types of chambers agree within 0.2% (as indicated by the error bars in Fig. 2), which is an evidence of the reliability of the method. It is interesting to point out that the results do not vary much for all three sources used (as indicated by the degree of overlap of the data points in Fig. 2). This implies that the scattering conditions for all the three beams are very similar. The contribution from scattered radiation is within the acceptable value of 5% specified in the recommendations of the International Organization for Standardization (ISO, 1996).

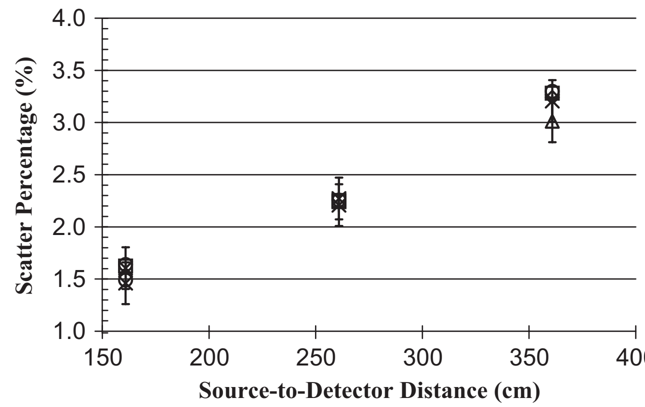

Fig. 2. Percentage of the scattered radiation relative to the total air-kerma value for three source-to-detector distances. The chamber A7 was used for the measurements made with the sources that have nominal activities of 300 mCi (diamonds) and 6 Ci (triangles). The PIC2 chamber was used for the measurements made with the sources that have nominal activities of 15 mCi (squares), 300 mCi (circles) and 6 Ci (crosses).

5. Conclusions

A calibration range was developed that provides air-kerma rates between 1.8 μGy/h (0.2 mR/h) and 5.3 mGy/h (0.6 R/h). Large-volume chambers were used to determine the air-kerma rates from three ^{137}Cs sources with initial nominal activities of 15 mCi, 300 mCi and 6 Ci (on October 15, 1994) at distances from the source between 1 and 4 m. Although these chambers have very different characteristics, an agreement within 0.3% between the rates determined with all of these chambers has been found. This agreement can be expected when similar types of chambers are used to characterize γ-ray beams at secondary standard calibration facilities. In addition, for the lowest air-kerma rate values, the uncertainty of the measured air-kerma rates obtained with the pressurized chambers (~1.1%) is lower than the uncertainty obtained with the non-pressurized chambers (~2.6%). As expected, for both chambers, the uncertainty decreases at the highest air-kerma rates measured, reaching a common value of 1%.

References

ANSI/NCSL Z540-2-1997, 1997. US guide to the expression of uncertainty in measurement, American National Standard for Expressing Uncertainty (NCSL, Boulder, CO).

Attix, F.H., 1986. Introduction to Radiological Physics and Radiation Dosimetry. Wiley, New York, pp. 38–79.

Boag, J.W., 1987. Ionization chambers. In: Kase, K.R., Bjärngard, B.E., Attix, F.H. (Eds.), The Dosimetry of Ionizing Radiation, Vol. II. Academic, New York, pp. 169–244.

Boutillon, M., 1998. Volume recombination parameter in ionization chambers. Phys. Med. Biol. 43, 2061–2072.

IAEA/SSDL Newsletter, 2005. Report of the 11th Meeting of the Secondary Standards Dosimetry Laboratories (SSDL) Scientific Committee, SSDL Newsletter No. 50 (IAEA, Vienna).

ISO-4037-1:1996(E), 1996. X and gamma reference radiation for calibrating dosimeters and dose rate meters for determining their response as a function of photon energy, Geneva.

Kafala, S.I., MacMahon, T.D., Gray, P.W., 1994. Testing of data evaluation methods. Nucl. Inst. Meth. A 339, 151–157.

Kondo, S., Randolf, M.L., 1960. Effect of finite size of ionization chambers on measurements of small photon sources. Radiat. Res. 13, 37–60.

Lamperti, P., O'Brien, M., 2001. Calibration of X-ray and gamma-ray measuring instruments, NIST Special Publication, pp. 250–258.

Loftus, T.P., Weaver, J.T., 1974. Standardization of ^{60}Co and ^{137}Cs gamma-ray beams in terms of exposure. J. Res. Nat. Bur. Stand. 78A, 465–476.

Minniti, R., Chen-Mayer, H., Seltzer, S.M., Saiful-Huq, M., Dewerd, L., Micka, J., Bryson, L., Slowey, T., Hanson, W., Wells, N., 2006. The US radiation dosimetry standards for ^{60}Co therapy level beams, and the transfer to the AAPM accredited dosimetry calibration laboratories. Med. Phys. 33 (4), 1074–1077.

Pibida, L., Minniti, R., O'Brien, M., Unterweger, M., 2005. Test of radiation detectors used in homeland security applications. Health Phys. 88 (Suppl. 2), 84–90.

Seltzer, S.M., Bergstrom, P.M., 2003. Changes in the US primary standards for the air kerma from gamma-ray beams. J. Res. Natl. Inst. Stand. Technol. 108, 359–381.

Sonzogni, A., 2006. National Nuclear Data Center, Brookhaven National Laboratory, 〈http://www.nndc.bnl.gov/nudat2〉.

Taylor, B.N., Kuyatt, C.E., 1994. Guidelines for evaluating and expressing the uncertainty of NIST measurement results. Natl. Inst. Stand. Technol., Technical note 1297.

Verhaegen, F., Van Dijk, E., Thierens, H., Aalbers, A., Seuntjens, J., 1992. Calibration of low activity ^{192}Ir brachytherapy sources in terms of reference air-kerma rate with large volume spherical ionization chambers. Phys. Med. Biol. 37 (11), 2071–2082.

Zankowski, C., Podgorsak, E.B., 1998. Determination of saturation charge and collection efficiency for ionization chambers in continuous beams. Med. Phys. 25 (6), 908–915.